



CHORUS

This is the accepted manuscript made available via CHORUS. The article has been published as:

Strongly driven molecules: Traces of soft recollisions for intermediate intensities in the over-the-barrier regime

A. Emmanouilidou and D. S. Tchitchekova

Phys. Rev. A **84**, 033407 — Published 12 September 2011

DOI: [10.1103/PhysRevA.84.033407](https://doi.org/10.1103/PhysRevA.84.033407)

Strongly driven molecules: traces of “soft” re-collisions for intermediate intensities in the over-the-barrier regime

A. Emmanouilidou^{1,2} and D. S. Tchitchekova²

*Department of Physics and Astronomy, University College London,
Gower Street, London WC1E 6BT, United Kingdom*¹

*and Chemistry Department, University of Massachusetts at Amherst, Amherst, Massachusetts, 01003, U.S.A.*²

Using a three-dimensional quasiclassical technique we explore double ionization in N_2 when driven by a linearly polarized, infrared (800 nm) long (27 fs) laser pulse. For intensities ranging from the tunneling to the over-the-barrier regime we identify the double ionization pathways in a unified way as a function of total final electron energy. Moreover, for intermediate intensities in the over-the-barrier regime we find that the correlated electron momenta have a prevailing square pattern. This square pattern is mainly due to the Delayed (one electron is ejected with a delay after re-collision) pathway’s contribution to double ionization. For intermediate intensities the Delayed pathway is dominated by “soft” re-collisions, first identified in Phys. Rev. A **80**, 053415 (2009), with the first electron tunneling at large field phases. We expect this square pattern to be absent for high intensities.

PACS numbers: 33.80.Rv, 34.80.Gs, 42.50.Hz

I. INTRODUCTION

Over the past two decades electron correlation has been established as the underlying mechanism for many important phenomena arising from the interaction of intense infrared laser pulses with matter. One of these phenomena is the dramatically enhanced multiple ionization yield of atoms (e.g. [1]) and molecules (e.g. [2]) for intensities where non-sequential double ionization (NSDI) dominates. For larger field intensities the two electrons are stripped out sequentially [3].

According to the accepted mechanism for NSDI—the three-step or re-scattering model [4]—1) one electron escapes through the field-lowered Coulomb potential, 2) it moves in the strong infrared laser field and 3) it returns to the core (possibly multiple times) to transfer energy to the other electron in the parent atomic or molecular ion. Using coincidence imaging techniques such as COLTRIMS many experiments have succeeded in obtaining highly differential kinematical details of electron correlation in the non-sequential intensity regime (e.g. [5–11]). The majority of theoretical work has concentrated on the non-sequential intensity regime (e.g. [12–14]). However, very interesting effects can also arise for intensities in the over-the-barrier regime such as an anti-correlation pattern with the electrons escaping in opposite directions for short laser pulses [15].

Here, we report on a classical study of electron correlation in the N_2 molecule driven by a long, 27 fs, laser pulse at 800 nm for intensities well within the non-sequential double ionization regime as well as for intermediate intensities in the over-the-barrier regime. We use the term intermediate for the intensities in the over-the-barrier regime where the majority of double ionizing trajectories are initiated with the tunneling model. We use a three-dimensional quasiclassical technique that we developed for the strongly driven He atom [16] and subsequently generalized for the strongly driven N_2 molecule

[15]. Our method is numerically very efficient and treats the Coulomb singularity with no approximation.

We first describe in a unified way the different double ionization (DI) pathways the two electrons follow to escape after re-collision as a function of total electron energy. (Throughout this work the total electron energy we refer to is the sum of the final kinetic energies of the two electrons). A similar description was very recently used to describe the DI pathways of strongly driven He [17, 18]. This general treatment allows us to identify universal features of strongly-driven molecular double ionization and compare them with the atomic case.

Moreover, we show that for intermediate intensities in the over-the-barrier regime “soft” re-collisions [15] with the re-colliding electron tunneling at large phases and a small transfer of energy to the initially bound electron underlie both the Direct and Delayed pathway of DI. These “soft” re-collisions give rise to an anti-correlation pattern, first identified for short laser pulses in ref. [15], in the correlated momenta of the Direct pathway of DI—simultaneous ejection of both electrons. We show that in the Delayed pathway—ejection of one electron with a delay of more than a quarter of a laser cycle after re-collision—“soft” re-collisions give rise to a square pattern. When the Direct pathway contributes the most to DI, indeed the case for short laser pulses [15], then the anti-correlation pattern prevails in the correlated momenta. In contrast, for long laser pulses the Delayed pathway contributes the most to DI and thus the square pattern prevails in the correlated momenta. The square pattern is expected to be absent for high intensities in the over-the-barrier regime.

II. METHOD

The method we use was previously described in [15]. For completeness we also describe it in what follows. Our

3-d quasiclassical model entails the following steps: We first set-up the initial phase space distribution of the two “active” electrons in the N_2 diatomic molecule. Here, we consider only parallel alignment between the molecular axis and the laser electric field. At intensities in the tunneling regime we assume that one electron tunnels through the field-lowered Coulomb potential. For the tunneling rate one can use quantum mechanical or semiclassical formulas for diatomic molecules (see, e.g. [19–22]). We use the rate provided in ref. [22]. The longitudinal momentum is zero while the transverse one is provided by a Gaussian distribution [23]. This description is valid as long as the potential barrier is not completely suppressed by the instantaneous laser field $E(t) = E_0(t) \cos(\omega t)$. We consider the usual laser wavelength of 800 nm, corresponding to $\omega = 0.057$ a.u. (a.u. - atomic units). In our simulation the pulse envelope $E_0(t)$ is defined as $E_0(t) = E_0$ for $0 < t < 7T$ and $E_0(t) = E_0 \cos^2(\omega(t - 7T)/12)$ for $7T < t < 10T$ with T the period of the field. The threshold for over-the-barrier ionization in neutral N_2 , with an ionization energy of $I_{p1} = 0.5728$ a.u., is reached at a field strength of $E = 0.075$ a.u. (corresponding to roughly 2×10^{14} Watts/cm²).

Above 2×10^{14} Watts/cm² the laser field allows an unhindered electron escape and therefore the initial phase space is modeled by a double electron microcanonical distribution [24]. However, in setting-up the initial phase space distribution we transition smoothly from the tunneling to the over-the-barrier intensity regime. Namely, we assign a random number to the phase ϕ of the laser field when the first electron is ionized, see [25, 26]. If the phase ϕ corresponds to an instantaneous strength of the laser field $E(\phi)$ that leaves the electron below the barrier then we use the initial conditions dictated by the tunneling model. If the instantaneous field strength pushes the barrier below the I_{p1} of that electron then we use the microcanonical distribution to set-up the initial phase space distribution. This choice of initial conditions has proven successful in past studies [26] in modeling the experimental ratio of double versus single ionization for long laser pulses [27]. With our approach we ensure a smooth transition of the initial phase space distribution as we change the intensity. Even at an intensity of 3×10^{14} Watts/cm² still about 70% of the double ionization probability corresponds to trajectories initialized using the tunneling model (thus the term intermediate intensities), while 30% of the probability corresponds to trajectories initialized using the microcanonical distribution.

After setting-up the initial phase space distribution we transform to a new system of coordinates, the so called “regularized” coordinates [28]. This transformation is exact and explicitly eliminates the Coulomb singularity. This step is more challenging for molecular systems since one has to “regularize” with respect to more than one atomic centers versus one atomic center for atoms. We regularize using the global regularization scheme described in ref. [29]. Finally, we use the Classical Trajectory Monte Carlo (CTMC) method for the time propa-

gation [30]. The propagation involves the 3-d four-body Hamiltonian in the laser field with “frozen” nuclei:

$$H = \sum_{i=1}^2 \left[\frac{p_i^2}{2} - \frac{1}{|\vec{R}/2 - \vec{r}_i|} - \frac{1}{|-\vec{R}/2 - \vec{r}_i|} \right] + \frac{1}{|\vec{r}_1 - \vec{r}_2|} + (\vec{r}_1 + \vec{r}_2) \cdot \vec{E}(t),$$

where $E(t)$ is the laser electric field polarized along the z direction and further defined as detailed above, and \vec{R} is the internuclear distance.

III. RESULTS AND DISCUSSION

We consider three laser intensities at 10^{14} , 1.5×10^{14} and 3×10^{14} Watts/cm². The range of laser intensities we consider is important because, at 800 nm, for 1.44×10^{14} Watts/cm² the maximum return energy of the re-colliding electron (3.2 U_p according to the three-step model [4]) equals the first ionization energy of the ground state of N_2^+ . The ponderomotive energy $U_p = E_0^2/(4\omega^2)$ is the cycle-averaged energy of the oscillatory motion.

A. Double ionization probability distribution

In this section we explore the prevalence of the different DI pathways as a function of total electron energy and intensity.

To identify the main DI energy transfer pathways we use the time delay between the re-collision time and the time of ionization of each electron [15]. We define the re-collision time as the time of minimum approach of the two electrons. We identify this time through the maximum in the electron pair potential energy. The ionization time for each electron is defined as the time when the sum of the electron’s kinetic energy (using the canonical momentum) and potential energy with the two atomic centers becomes positive and remains positive thereafter—for more details for the time of ionization see [16] and references there in.

Following the steps outlined above, we identify the following pathways: the Direct and Delayed which are well established. (The delayed pathway is also referred to as re-collision-induced excitation with subsequent field ionization, RESI [31, 32]). In the Direct ionization pathway (SE) both electrons are ionized simultaneously very close (less than a quarter of a laser period) to the re-collision time. In the Delayed ionization pathway, the re-colliding electron excites the remaining electron but does not ionize it. The electron is subsequently ionized at a peak (RESIa) or at a zero (RESIb) of the laser electric field. In addition to the SE and RESI pathways we also identify the double delayed ejection pathway (DDE) with both electrons ionizing more than a quarter of a laser cycle after re-collision. This pathway was first identified in our recent study of strongly driven He [18].

% contribution of DI pathways. In Fig. 1, top row, we plot the probability distribution of DI for 10^{14} , 1.5×10^{14} and 3×10^{14} Watts/cm². Moreover, for each intensity, we plot the % contribution of each DI pathway as a function of the total electron energy, see bottom row in Fig. 1. We use energy steps as small as the immense computational challenge of the endeavor allows—1-2 million DI events for the whole energy regime.

a) Small total energies. For small intensities the DDE pathway prevails for small total electron energy with a % contribution changing from 80% for 10^{14} Watts/cm² to 30% for 3.0×10^{14} Watts/cm². We find that for N₂ in the DDE pathway the re-colliding electron does not get significantly trapped by the core after re-collision and thus the two electrons do not escape in opposite directions as is the case for strongly driven He, see [18]. A possible explanation is that the presence of two nuclear centers instead of one with nuclear charge of one instead of two (He charge) makes it harder for the re-colliding electron to become bound after re-collision. As the intensity increases to 3.0×10^{14} Watts/cm² crossing over to the over-the-barrier regime, for small total energy, the sequential ionization (SI) pathway takes over. We define SI as the pathway where there is no re-collision and both electrons ionize mainly due to their individual interaction with the laser field.

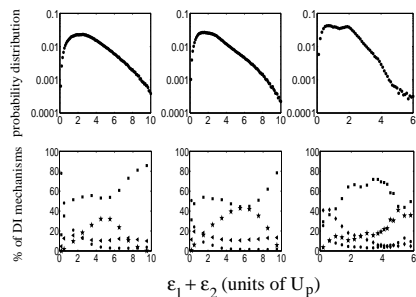


FIG. 1. Top row: Double ionization probability distribution; Bottom row: % contributions of the main DI mechanisms (● for DDE, ◀ for RESIa, ■ for RESIb, ★ for SE). First column: 10^{14} Watts/cm², second column: 1.5×10^{14} Watts/cm², third column: 3×10^{14} Watts/cm² (at this intensity an additional DI mechanism appears, the SI mechanism, given by ◆). Note that for 3×10^{14} Watts/cm² we only show the combined contribution of RESIa and RESIb.

b) Intermediate and high total energies. For all intensities considered, the Delayed pathway prevails for all energies, with the exception of very small ones. The % contribution of SE is always smaller than that of the RESI’s. A trace of collisional physics on strong field ionization is the overall shape of the SE contribution to DI as a function of total energy. It is very small for small and high energies while it is large for intermediate energies, as we have already found for strongly driven He [18]. Thus, SE qualitatively resembles electron impact ionization.

For strongly driven He, RESI prevails independent of the total electron energy [17] for intensities where $3.2 U_p$

is below the first excitation energy of He⁺. For higher intensities, for strongly driven He, the SE pathway prevails for intermediate total electron energy, see [17, 18]. In contrast, for strongly driven N₂, RESI prevails for all intensities. The larger contribution of RESI to strongly driven N₂, possibly, arises because the interaction of the field with the molecular ion makes available a much larger number of excited states to the bound electron compared to the atomic case. Upon return of the re-colliding electron to the molecular ion, electron 2 can be found in any of these excited states. It is thus less probable for electron 2 to interact strongly with electron 1 and escape through SE; it is more probable for electron 2 to gain some energy from the re-colliding electron, get further excited, and subsequently ionize through RESI.

We also note, that the % contribution of different DI pathways depends on the duration of the pulse. In the current work RESI prevails for strongly driven N₂ because of the long duration of the laser pulse. For shorter duration pulses it is the Direct pathway that prevails. [15].

B. Traces of “soft” re-collisions in the DI probability distribution

For intermediate intensities in the over-the-barrier regime, 3×10^{14} Watts/cm², we find that the probability for both electrons to ionize with a large total energy is smaller than for intensities in the tunneling regime, see Fig. 1. This is expected since with increasing intensity transfer of energy from electron 1—the one that tunnels in the initial state—to electron 2 through “hard” re-collisions is less probable. Moreover, we find that for intermediate intensities in the over-the-barrier regime the DI probability distribution has two peaks. From the energy sharing between the two electrons, see double differential in energy in Fig. 2, we find that for the peak present for smaller intensities the two electrons share the energy in all possible ways. This is consistent with the presence of “hard” re-collisions where the two electrons can share the energy in many possible ways after re-collision. We identify this same pattern of energy sharing between the two electrons for the peak at smaller total energies for 3×10^{14} Watts/cm². This shift of the peak towards smaller energies with increasing intensity is consistent with the less efficient transfer of energy from electron 1 to 2.

A clear signature of this less efficient transfer of energy is as we now show the second peak, the one at higher total energies, $1.9 U_p$, for 3×10^{14} Watts/cm², see Fig. 1. From Fig. 2 (bottom row) we find that, when the total energy is between 1.6 - $2.4 U_p$, the two electrons share the energy asymmetrically. We find that electron 1 (re-colliding) escapes with most of the energy. Furthermore, we plot in Fig. 3 for each DI pathway the probability for each electron to escape with a certain amount of final energy. The re-colliding electron’s RESI probability distribution shown in Fig. 3 varies smoothly as a func-

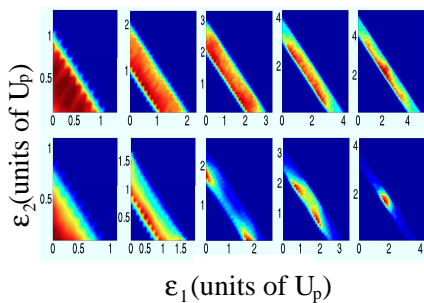


FIG. 2. Double differential probability in energy: top row for 10^{14} Watts/cm² for the energy intervals $(0,1)U_p$, $(1,2)U_p$, $(2,3)U_p$, $(3,4)U_p$ and $(4,5)U_p$; bottom row for 3×10^{14} Watts/cm² for $(0,0.8)U_p$, $(0.8,1.6)U_p$, $(1.6,2.4)U_p$, $(2.4,3.2)U_p$ and $(3.2,4)U_p$.

tion of the electron’s final energy for intensities in the tunneling regime (bottom row); in contrast, it has a pronounced peak around $1.6 U_p$ for 3×10^{14} Watts/cm² (top row). We thus find that it is the re-colliding electron’s RESI probability distribution that accounts for the peak at higher total energy in the total DI probability distribution in Fig. 1.

We now show that the peak at $1.6 U_p$ of the re-colliding electron’s RESI distribution is related to “soft” re-collisions. Indeed, electron’s 1 final energy of $1.6 U_p$ corresponds to the momentum at the tunneling time when the field phase is $50\text{-}60^\circ$ for the RESI pathway, see Fig. 4 b). Large tunneling phases result in short trajectories where electron 1 acquires a smaller amount of energy from its excursion in the laser field before returning back to the nuclei and thus transfers a smaller amount of energy to electron 2, “soft” re-collisions. The re-collision is particularly “soft” for the Delayed pathway where for 70% of the events electron 1 ionizes much earlier than the re-collision time. We find that the percentage contribution of these particularly “soft” re-collisions increases monotonically as a function of final electron energy reaching its maximum value for an electron energy at and above $1.6 U_p$.

We expect this second peak in the DI probability distribution to be present only for intermediate intensities. The reason is that as we have shown this second peak stems from the presence of the “soft” re-collisions. However, for small intensities the tunneling phase of electron 1 is peaked close to the maximum of the laser field (zero phase) resulting in “hard” re-collisions. In addition, for high intensities the SI pathway prevails and the electrons are driven sequentially away from the core—most probably at large negative field phases as shown in Fig. 4 c). This results in two equivalently ionizing electrons which is not consistent with the asymmetric energy sharing observed for the second peak in the DI probability distribution for 3×10^{14} Watts/cm².

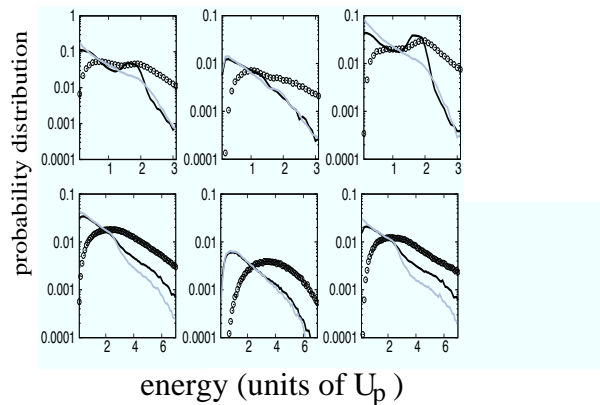


FIG. 3. Top row 3×10^{14} Watts/cm², first column from the left: total DI probability distribution as a function of total energy (circles) and probability distribution as a function of one electron’s final energy, for the re-colliding electron (black line) and for electron 2 (grey line). Second and third column same as the first but for the SE and RESI pathways. Bottom row, same as top row but for 10^{14} Watts/cm².

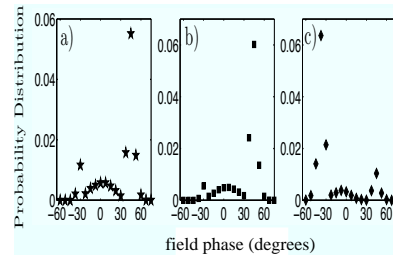


FIG. 4. Field phase when electron 1 tunnels for the a) SE, b) the RESI and c) the SI pathways at 3×10^{14} Watts/cm².

C. Traces of “soft” re-collisions in the correlated momenta

In this section, we explore the traces of the “soft” re-collisions in the correlated momenta at an intensity 3×10^{14} Watts/cm².

In Fig. 5 we show the correlated momenta of the two electrons for the SE, RESIa, RESIb pathways as well as for all DI pathways combined. We find that the RESIa and RESIb pathways have distinct patterns only for 10^{14} and 1.5×10^{14} Watts/cm² while for 3×10^{14} Watts/cm² they are almost indistinguishable. Since for 3×10^{14} Watts/cm² there is no real distinction between RESIa and RESIb we only show the combined contribution of the Delayed pathway for this high intensity.

The SE correlated momenta have a pronounced anti-correlation pattern as shown in Fig. 5 for 3×10^{14} Watts/cm². For the majority of SE trajectories the re-colliding electron tunnels at a phase around 50° , see Fig. 4 a), giving rise to “soft” re-collisions. 30% of these re-collisions are particularly “soft” with the re-colliding electron ionizing at an early time before re-collision (we

find the re-collision time to be $T/2$); the second electron ionizes just after re-collision. Thus the two electrons ionize at times corresponding to opposite signs of the vector potential resulting in opposite final electron momenta. For the remaining of SE events both electrons ionize mostly after $T/2$. For some of these latter DI events the two electrons escape in the same direction, as is the case in the tunneling regime for 10^{14} Watts/cm² and 1.5×10^{14} Watts/cm². However, for others, the small amount of energy transfer from electron 1 to electron 2 and possibly the Coulomb repulsion, result in the two electrons escaping in opposite directions. Overall electrons escaping in opposite directions is the biggest contribution to SE giving rise to an anti-correlation pattern. For short laser pulses the SE pathway contributes the most to DI and thus the anti-correlation pattern prevails in the correlated momenta [15].

We further note that at 3×10^{14} Watts/cm² the correlated momenta of the Delayed pathway have a pronounced square structure, see Fig. 5. This feature can be understood again in terms of the “soft” re-collisions that underly DI. As discussed in the previous section, for 70% of the RESI trajectories re-collisions are particularly “soft” with the re-colliding electron ionizing much earlier than the re-collision time. For the latter trajectories the final momentum of the re-colliding electron (corresponding to a final energy of $1.6 U_p$) is mostly determined by the vector potential at the time the electron tunnels out. The momentum of electron 1 at the tunneling time corresponds to the boundary of the square pattern. For long laser pulses the RESI pathway contributes the most to DI, as we have shown in section A, and thus the square pattern prevails in the correlated momenta [15].

Thus, the square pattern in the correlated momenta can be understood in terms of the “soft” re-collisions. The main feature of the “soft” re-collisions is tunneling of electron 1 in the initial state at large field phases. Since the latter holds true only at intermediate intensities (see discussion at the end of the previous paragraph) one does not expect that the square pattern survives at high intensities.

IV. CONCLUSIONS

We have explored in detail the prevalence of the DI pathways for strongly driven N₂ for intensities ranging from the tunneling to the over-the-barrier regime. We

have found that the Delayed pathway prevails for all intensities and for all total energies, with the exception of very small ones. This differs from strongly driven He where the SE pathway prevails for intermediate total energies for higher intensities (intensities where $3.2 U_p$ is above the first excitation energy of He⁺).

For intermediate intensities in the over-the-barrier regime, we have found that “soft” re-collisions underly both the Direct and the Delayed pathway of DI. In these “soft” re-collisions electron 1 tunnels at a large phase

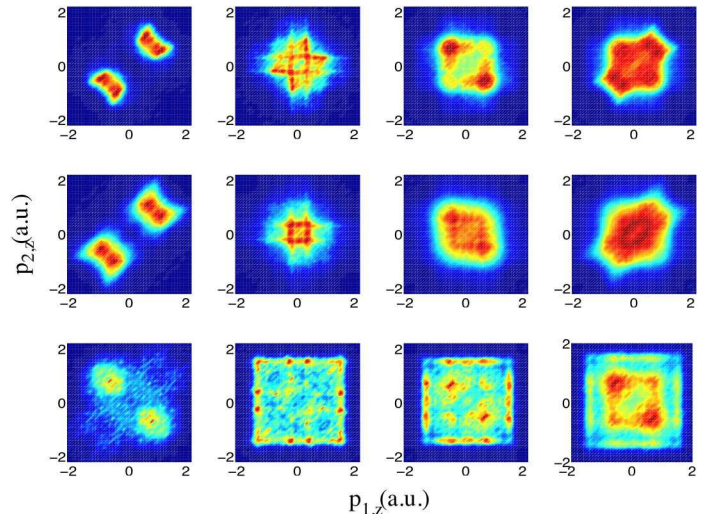


FIG. 5. Correlated momenta at intensities 10^{14} Watts/cm² (top row), 1.5×10^{14} Watts/cm² (middle row), and 3×10^{14} Watts/cm² (bottom row). Columns from left to right indicate the various DI mechanisms: SE, RESIa, RESIb, and the contribution of all DI mechanisms combined.

of the laser field, has a small maximum excursion in the laser field, and upon its return to the molecular ion transfers a small amount of energy to electron 2. These “soft” re-collisions give rise to a square pattern in the correlated momenta for the Delayed pathway and an anti-correlation pattern for the Direct pathway. Both the anti-correlation and the square pattern are experimentally accessible. For higher intensities in the over-the-barrier regime re-collisions disappear and sequential ionization prevails. Both electrons escape in an equivalent way which is not consistent with a square pattern in the correlated momenta.

-
- [1] B. Walker, B. Sheehy, L.F. DiMauro, P. Agostini, K.J. Schafer, and K.C. Kulander, Phys. Rev. Lett. **73**, 1227 (1994).
 [2] A.S. Alnaser, T. Osipov, E.P. Benis, A. Wech, B. Shan, C.L. Cocke, X.M. Tong, and C.D. Lin, Phys. Rev. Lett. **91**,163002 (2003).
 [3] P. Lambropoulos, Phys. Rev. Lett. **55**, 2141 (1985).

- [4] P.B. Corkum, Phys. Rev. Lett. **71**, 1994 (1993).
 [5] Th. Weber, H. Giessen, M. Weckenbrock, G. Urbasch, A. Staudte, L. Spielberger, O. Jagutzki, V. Mergel, M. Vollmer, and R. Dörner, Nature **405**, 658 (2000).
 [6] E. Eremina, X. Liu, H. Rottke, W. Sandner, A. Dreischuh, F. Lindner, F. Grasbon, G.G. Paulus, H. Walther, R. Moshhammer, B. Feuerstein, and J. Ullrich, J. Phys. B

- 36**, 3269, 2003.
- [7] V.L.B. de Jesus, A. Rudenko, B. Feuerstein, K. Zrost, C.D. Schröter, R. Moshhammer, and J. Ullrich, *J. Elec. Spect. Rel. Phen.* **141**, 127 (2004).
- [8] M. Weckenbrock, D. Zeidler, A. Staudte, Th. Weber, M. Schöffler, M. Meckel, S. Kammer, M. Smolarski, O. Jagutzki, V. R. Bhardwaj, D. M. Rayner, D. M. Villeneuve, P. B. Corkum, and R. Dörner, *Phys. Rev. Lett.* **92**, 213002 (2004).
- [9] A. Staudte, C. Ruiz, M. Schöffler, S. Schössler, D. Zeidler, Th. Weber, M. Meckel, D.M. Villeneuve, P.B. Corkum, A. Becker, and R. Dörner, *Phys. Rev. Lett.* **99**, 263002 (2007).
- [10] A. Rudenko, V.L.B. de Jesus, Th. Ergler, K. Zrost, B. Feuerstein, C.D. Schröter, R. Moshhammer, and J. Ullrich, *Phys. Rev. Lett.* **99**, 263003 (2007).
- [11] Yunquan Liu, S. Tschuch, A. Rudenko, M. Dürr, M. Siegel, U. Morgner, R. Moshhammer, and J. Ullrich, *Phys. Rev. Lett.* **101**, 053001 (2008).
- [12] P.J. Ho, *Phys. Rev. A* **72**, 045401 (2005).
- [13] S.L. Haan, L. Breen, A. Karim, and J.H. Eberly, *Phys. Rev. Lett.* **97**, 103008 (2006).
- [14] D.Y. Bondar, Wing-Ki Liu, and M.Yu. Ivanov, *Phys. Rev. A* **79**, 023417 (2009).
- [15] A. Emmanouilidou and A. Staudte, *Phys. Rev. A* **80**, 053415 (2009).
- [16] A. Emmanouilidou, *Phys. Rev. A* **78**, 023411 (2008).
- [17] A. Emmanouilidou, J. S. Parker, L. R. Moore and K. T. Taylor, *New Journal of Physics* **13**, 043001 (2011).
- [18] A. Emmanouilidou, *Phys. Rev. A* **83**, 023403 (2011).
- [19] X.M. Tong, Z.X. Zhao, and C.D. Lin, *Phys. Rev. A* **66**, 033402 (2002).
- [20] I.V. Litvinyuk, K.F. Lee, P.W. Dooley, D.M. Rayner, D.M. Villeneuve, and P.B. Corkum, *Phys. Rev. Lett.* **90**, 233003 (2003).
- [21] T.K. Kjeldsen and L.B. Madsen, *J. Phys. B* **37**, 2033 (2004).
- [22] Y. Li, J. Chen, S.P. Yang, and J. Liu, *Phys. Rev. A* **76**, 023401 (2007).
- [23] J. Liu, D.F. Ye, J. Chen, and X. Liu, *Phys. Rev. Lett.* **99**, 0113003 (2007).
- [24] L. Meng, C.O. Reinhold, and R.E. Meng, *Phys. Rev. A* **40**, 3637 (1989).
- [25] T. Brabec, M. Ivanov, and P.B. Corkum, *Phys. Rev. A* **54**, R2551 (1996).
- [26] D.F. Ye, X. Liu, and J. Liu, *Phys. Rev. Lett.* **101**, 233003 (2008).
- [27] C. Cornaggia and Ph. Hering, *Phys. Rev. A* **62**, 023403 (2000).
- [28] P. Kustaanheimo and E. Stiefel, *J. Reine Angew. Math.* **218**, 204 (1965).
- [29] D.C. Hoggie, *Celestial Mechanics* **10**, 217 (1974).
- [30] R. Abrines and I.C. Percival, *Proc. Phys. Soc.* **89**, 515 (1966).
- [31] R. Kopold, W. Becker, H. Rottke and W. Sandner, *Phys. Rev. Lett.* **85**, 3781 (2000).
- [32] B. Feuerstein, R. Moshhammer, D. Fischer, A. Dorn, C. D. Schröter, J. Deipenwisch, J. R. Crespo Lopez-Urrutia, C. Höhr, P. Neumayer, J. Ullrich, H. Rottke, C. Trump, M. Wittmann, G. Korn, and W. Sandner, *Phys. Rev. Lett.* **87**, 043003 (2001).